

## 科技关注

氯化胆碱-尿素离子液体中镁合金  
表面电沉积电流密度对镀锌层性能的影响王 巍<sup>1,2</sup>, 初青伟<sup>1</sup>, 梁 军<sup>1</sup>, 戴剑锋<sup>2</sup>

(1. 中国科学院兰州化学物理研究所 固体润滑国家重点实验室, 甘肃 兰州 730000;

2. 兰州理工大学理学院, 甘肃 兰州 730000)

**[摘要]** 为了提高 AM60B 镁合金的耐腐蚀性能,以氯化胆碱-尿素(Reline)离子液体为电镀液,在 AM60B 镁合金表面脉冲电镀锌。利用扫描电镜、能谱仪、X 射线衍射仪及涂层厚度测量仪研究了电沉积电流密度对镀锌层微观形貌及结构的影响;采用电化学极化曲线测试了不同电流密度下所得镀锌层的耐腐蚀性能。结果表明:随着电流密度的增加,镀锌层的晶粒逐渐变大,孔洞等缺陷减少,耐腐蚀性能先增强后减弱;当电流密度为 5.0 mA/cm<sup>2</sup>时,镀锌层均匀致密、光亮、无明显缺陷、与基体结合力好、耐腐蚀性能最佳。

**[关键词]** 电镀锌层; AM60B 镁合金; 氯化胆碱-尿素离子液体; 电流密度; 结合力; 耐蚀性

**[中图分类号]** TQ153.1+5

**[文献标识码]** A

**[文章编号]** 1001-1560(2013)08-0001-04

## 0 前言

镁合金比强度高、密度小、热导率较高、尺寸稳定性高、电磁屏蔽特性好、阻尼性和切削加工性能良好、易回收,在汽车、计算机、航空航天、手机、运动器材、手持工具和家用设备中广泛应用。但镁合金化学活性高、耐蚀性、耐磨性和抗蠕变性能差,制约了其应用。镁合金表面电镀锌可以显著提高其耐蚀性,同时也可作为后续处理的底层。氰化镀锌溶液均镀能力好,镀层光亮细致,但存在对环境污染严重、电镀需在高温下进行、镀液导电性较差、电流效率低、电镀过程因析氢会降低镀层抗拉强度等缺陷。无氰镀液稳定、成本低、无污染、电流效率高,但对试样有腐蚀作用,均镀能力和深镀能力较差,镀层结晶较粗,镀层的结合力和脆性方面不及氰化镀锌。

离子液体具有蒸气压低、稳定性好、不挥发、无污染、无毒性、对有机和无机化合物溶解性好等优

点<sup>[1-4]</sup>;离子液体为全离子结构,具有良好的导电性,既可作溶剂,又可作电解质<sup>[5]</sup>。就电沉积而言,离子液体兼具了高温熔融盐和水溶液的优点<sup>[6]</sup>:较宽的电化学窗口,有的高达 4 V,远高于水溶液的,在室温下就可以使沉积电势较负的金属和一些难以从水溶液体系中沉积出来的活泼金属如镁和锂从离子液体中沉积出来;提高了电沉积电流效率,有效避免了电解液的分解,还可避免析氢而产生的氢脆,副反应少,金属镀层质量更好<sup>[3,7-9]</sup>。此外,离子液体黏度较大、扩散速度慢、易获得纳米级金属粒子,使镀层晶粒细化,更加致密<sup>[10]</sup>。传统咪唑类和吡啶类离子液体存在制备繁琐、提纯困难、成本较高、产率低等缺点<sup>[3]</sup>,制约了其产业化进程。氯化胆碱-尿素(Reline)离子液体是一种低共熔混合物,具有离子液体的普遍性质,其在大气中稳定性好、容易获得、可循环使用、原材料便宜,不易造成化学污染<sup>[3,10]</sup>,不具腐蚀性。目前,电沉积锌镀层的研究主要在钢材上进行,在镁合金上的较少。有报道称从 Reline 离子液体中在镁合金上成功制备了电沉积锌层,考察了基体组成、前处理以及电流波形等对镀层形貌及耐腐蚀性能的影响<sup>[7,11]</sup>。结果表明,电流波形对镀层的质量与性能有重要影响,与常规直流电镀相比,脉冲电镀制备的镀锌层更加均匀致密,与基体的结合力更好,能更有效地提高镁合金的耐蚀性能。但上述研究未对脉冲电

**[收稿日期]** 2013-02-20

**[基金项目]** 中国科学院“百人计划”(Y00230YBR1)资助

**[通信作者]** 梁 军(1979-),研究员,博士,主要从事轻金属材料环境行为与表面工程的研究,电话:0931-4968381,E-mail:jliang@licp.cas.cn

镀工艺参数进行更系统深入的研究。

本工作采用 Reline 离子液体在镁合金表面脉冲电镀锌,重点研究了电流密度对镀锌层的晶粒尺寸、微观形貌、致密性和耐腐蚀性能的影响。

## 1 试验

### 1.1 基材前处理

基材为 AM60B 镁合金,成分(质量分数,%) : 95.40~95.60 Mg, 0.20 Al, 0.26~0.50 Zn, 余量为 Fe, 尺寸为 36 mm×20 mm×2 mm。预处理<sup>[7]</sup>: 打磨(用 800~2 000 号砂纸逐级打磨后,机械抛光至呈现金属光泽)→除油(40 g/L NaOH, 20 g/L Na<sub>2</sub>CO<sub>3</sub>, 30 g/L Na<sub>3</sub>PO<sub>4</sub>, 65 °C, 10 min)→酸洗[165 mL/L H<sub>3</sub>PO<sub>4</sub> (85%), 1 g/L Na<sub>2</sub>MoO<sub>4</sub>·2H<sub>2</sub>O, 45 °C, 15 s]→碱洗(80 g/L Na<sub>4</sub>P<sub>2</sub>O<sub>7</sub>, 20 g/L Na<sub>2</sub>CO<sub>3</sub>, 30 g/L NaNO<sub>3</sub>, 75 °C, 10 min)→活化[400 mL/L HF(40%), 室温]→浸锌(30 g/L ZnSO<sub>4</sub>·7H<sub>2</sub>O, 120 g/L Na<sub>4</sub>P<sub>2</sub>O<sub>7</sub>, 5 g/L NaF, 6 g/L Na<sub>2</sub>CO<sub>3</sub>, 75 °C, 10 min)→热风吹干;每步工艺之间用蒸馏水清洗试样。

### 1.2 Reline 离子液体电镀锌

(1) Reline 离子液体的配制 将氯化胆碱(99%, 分析纯)、尿素(99%, 分析纯)和 ZnCl<sub>2</sub> 按摩尔比 1.00:2.00:0.25 混合均匀,于控温磁力搅拌器中恒温 80 °C 加热并搅拌,至完全溶解,形成无色透明液体,即成 Reline 离子液体<sup>[12]</sup>。

(2) 电镀锌 设备为 SMD-30P 型多脉冲电镀电源;阳极为 80.0 mm×70.0 mm×0.1 mm 纯锌板,阴极 AM60B 镁合金,两电极间的距离为 70 cm;频率为 2 000 Hz,占空比为 3/4;时间为 120 min,温度为 80 °C;电流密度分别为 4.0、5.0、6.0 mA/cm<sup>2</sup>。镀完后用丙酮超声波清洗试样。

### 1.3 镀层性能测试

(1) 形貌、成分、结构及厚度 采用 JSM-5600LV 型低真空扫描电镜(SEM)及其自带的 X 射线能量色散谱(EDS)观察镀层的表面及截面形貌、分析其成分;采用 D/Max-2400 型粉末 X 射线衍射仪(XRD)分析镀层晶体结构;采用 fischer FMP40 涂层测厚仪测量镀层的厚度。

(2) 结合力 采用划痕法测试,选用含 6 个刀片的划刀(刀片间齿距为 1.0 mm)沿 45° 方向以十字交叉方式划去表面镀层,露出基体与镀层界面,形成栅格。然后用软刷轻刷镀层表面,以除去多余的碎屑。观察划痕处是否有起皮、剥落,以此判断镀层与基体的结合程度。

(3) 极化性能 采用 PGSTAT302N 型 AUTOLAB 电化学工作站测试极化曲线:腐蚀介质为 0.1 mol/L NaCl 溶液,参比电极为 Ag/AgCl 电极,辅助电极为铂片电极,工作电极为镀锌试样,有效工作面积为 0.5 cm<sup>2</sup>;测试在室温下进行,镀锌试样在腐蚀介质中浸泡 30 min 后再开始测试;扫描速度为 1 mV/s,扫描范围为 -1.8~-0.4 V。

## 2 结果与讨论

### 2.1 镀锌层的厚度、表面及截面形貌

图 1 为不同电流密度下所得镀锌层的表面 SEM 形貌。从图 1 可以看出:镀层主要由不规则的多边形晶粒组成,镀层均匀、平整,各晶粒之间排列紧密;随着电流密度的增大,晶粒尺寸也逐渐变大;当电流密度较大(6.0 mA/cm<sup>2</sup>)时,由于晶粒沉积速度较快,大晶粒较多,镀锌层疏松且边缘出现了发黑现象,而黑色部分的镀层与基体结合力极差;电流密度较小(4.0 mA/cm<sup>2</sup>)时,由于晶粒沉积速度较慢,镀层较薄,孔洞较多,晶粒局部堆积现象明显,导致镀层均匀性较差,甚至露出部分底材;电流密度为 5.0 mA/cm<sup>2</sup>时,晶粒堆积现象相对较弱,大晶粒也较少,所得镀层孔洞少、均匀致密、平整光亮。

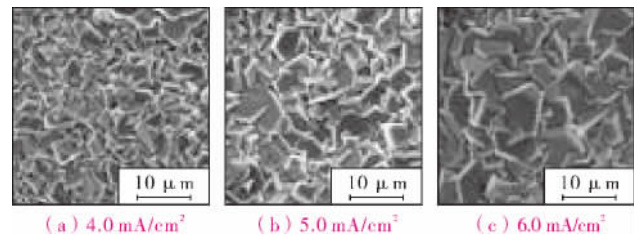


图 1 不同电流密度下镀锌层的表面 SEM 形貌

4.0、5.0、6.0 mA/cm<sup>2</sup> 电流密度下所得镀锌层的厚度分别为 23.0、23.9、24.3 μm。可见,不同电流密度下所得镀锌层的厚度差异不大,这是因为电流密度变化范围较小,对膜厚的影响较小。

图 2 为电流密度为 5.0 mA/cm<sup>2</sup> 时所得镀锌试样的截面 SEM 形貌。由图 2 可以看出,镀锌层厚度均匀、膜层平整致密,与基体紧密结合,未出现分层现象,这都有利于提高镀层的防护性能。

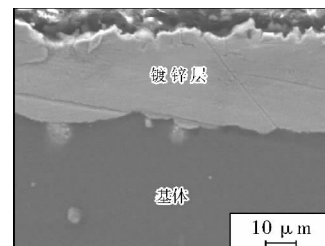


图 2 镀锌层试样的截面 SEM 形貌

## 2.2 镀锌层的成分

图3和图4分别为电流密度为 $5.0 \text{ mA/cm}^2$ 时, AM60B 镁合金表面镀锌层的EDS谱和XRD谱。图3显示, 镀层中锌的含量为100%。图4显示, 主要的衍射峰为Zn衍射峰, 同时还检测到了Mg衍射峰。Mg衍射峰的出现是因为X射线穿入较深, 到达了镁合金基体。由此可以确定, 得到的镀层是纯锌层。

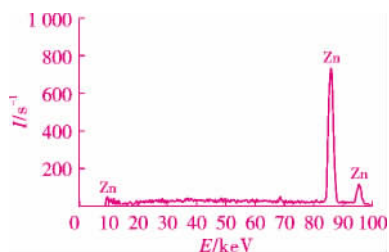


图3 镀锌层的EDS谱

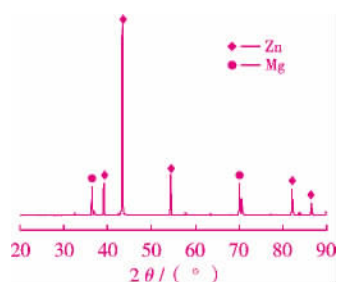


图4 镀锌层的XRD谱

## 2.3 镀锌层的结合力

图5为电流密度为 $5.0 \text{ mA/cm}^2$ 时所得镀锌层经结合力测试后划痕处的SEM形貌。从图5可以看出, 外力破坏痕迹周围的镀层无起皮、剥落或破裂现象, 说明镀锌层与镁合金基体结合紧密, 不易脱落。

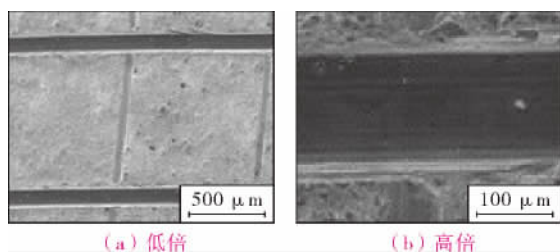


图5 结合力测试后镀锌层划痕处的SEM形貌

## 2.4 镀锌层的耐腐蚀性能

图6为不同电流密度下所得镀锌层、AM60B 镁合金及纯锌的动电位极化曲线, 表1为相应的电化学拟合参数。从图6可以看出: 5种试样的极化曲线具有相似的形状; 极化曲线的阴极区主要为析氢反应, 当电位正于腐蚀电位后, 进入阳极区, 腐蚀电流迅速增大, 随后进入钝化区, 电位超过一定值后, 发生过钝化, 电流再次迅速增大<sup>[1]</sup>。从表1可以看出: 电流密

度为 $4.0 \text{ mA/cm}^2$ 时, 镀锌试样的腐蚀电位 $E_{\text{corr}}$ 为 $-1415 \text{ mV}$ , 与镁合金基体的腐蚀电位相同, 腐蚀电流密度 $J_{\text{corr}}$ 由镁合金基体的 $1.78 \times 10^{-6} \text{ A/cm}^2$ 增大到 $2.13 \times 10^{-5} \text{ A/cm}^2$ , 说明此条件下, 镀锌层不仅没有为镁合金基体提供防护作用, 反而加速了其腐蚀; 电流密度为 $5.0 \text{ mA/cm}^2$ 时, 腐蚀电位 $E_{\text{corr}}$ 正移至 $-1306 \text{ mV}$ , 腐蚀电流密度 $J_{\text{corr}}$ 为 $8.07 \times 10^{-6} \text{ A/cm}^2$ , 镀锌层耐蚀性比 $4.0 \text{ mA/cm}^2$ 时明显提高, 且与纯锌较为接近; 电流密度为 $6.0 \text{ mA/cm}^2$ 时, 镀锌层的耐蚀性又有所降低。结合镀层表面形貌可知: 电流密度过小, 所沉积的晶粒较小, 晶粒局部堆积现象明显, 镀层孔洞较多, 有效厚度较薄, 镀锌层在腐蚀介质中浸泡一段时间后, 容易发生穿透性点蚀, 最终在镀锌层与基体之间形成腐蚀电偶, 加速了基体的腐蚀; 电流密度为 $5.0 \text{ mA/cm}^2$ 时, 均匀致密、缺陷少的镀锌层具有优异的耐腐蚀性能, 可为镁合金基体提供较好的防护作用; 电流密度过大时, 晶粒较大, 大晶粒多, 使得镀锌层相对疏松, 有效厚度略薄, 镀锌层不能为镁合金基体提供有效防护。

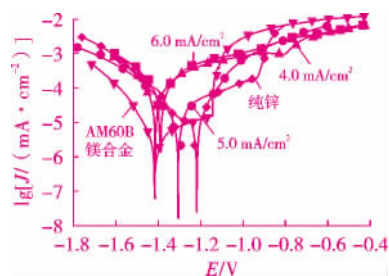


图6 AM60B 镁合金、镀锌层及纯锌的动电位极化曲线

表1 极化曲线的电化学参数

试样	$E_{\text{corr}}/\text{mV}$	$J_{\text{corr}}/(\text{A}\cdot\text{cm}^{-2})$
镀锌试样( $4.0 \text{ mA/cm}^2$ )	-1415	$2.13 \times 10^{-5}$
镀锌试样( $5.0 \text{ mA/cm}^2$ )	-1306	$8.07 \times 10^{-6}$
镀锌试样( $6.0 \text{ mA/cm}^2$ )	-1388	$1.77 \times 10^{-5}$
AM60B 镁合金	-1415	$1.78 \times 10^{-6}$
纯 Zn	-1216	$1.47 \times 10^{-6}$

## 3 结论

(1) Reline 离子液体中, 在 AM60B 镁合金表面脉冲电镀锌, 电流密度对镀锌层质量的影响较为明显, 随着电流密度的增加, 镀锌层颗粒逐渐变大, 晶粒堆积现象减弱, 大晶粒增多, 孔洞等缺陷减少, 镀锌层的耐腐蚀性能先增强后减弱。

(2) 当电流密度为 $5.0 \text{ mA/cm}^2$ 时, 镀锌层表面均匀致密、平整光亮、无明显缺陷, 耐腐蚀性能与纯锌相

近,可为 AM60B 镁合金基体提供较好的防护作用。

### [ 参 考 文 献 ]

- [ 1 ] Yang M H, Sun I W. Electrodeposition of antimony in a water-stable 1-ethyl-3-methylimidazolium chloridetetra-fluoroborate room temperature ionic liquid [J]. Journal of Applied Electrochemistry, 2003, 33(11): 1 077 ~ 1 084.
- [ 2 ] Hagiwara R, Ito Y. Room temperature ionic liquids of alkylimidazolium cations and fluoroanions [J]. Journal of Fluorine Chemistry, 2000, 105(2): 221 ~ 227.
- [ 3 ] 付雄之,于爱凤,顾建胜. 室温离子液体中电沉积金工艺研究 [M]. 材料保护, 2009, 42(2): 22 ~ 24.
- [ 4 ] Mukhopadhyay T, Freyland W. Electrodeposition of Ti nanowires on highly oriented pyrolytic graphite from an ionic liquid at room temperature [J]. Langmuir, 2003, 19(6): 1 951 ~ 1 953.
- [ 5 ] 王晓娟,李慧,王娇等. 钴锌合金在氯化胆碱-尿素离子液体中的电沉积行为 [J]. 材料保护, 2010, 43(3): 30 ~ 33.
- [ 6 ] Zhang S Y, Li Q, Chen B, et al. Electrodeposition of zinc on AZ91D magnesium alloy pre-treated by stannate conversion coatings [J]. Materials Corrosion, 2010, 61(10): 860 ~ 865.
- [ 7 ] 杨海燕,郭兴伍,吴国华,等. AZ91D 镁合金在氯化胆碱-尿素离子液体中电沉积 Zn 的研究 [J]. 中国腐蚀与防护学报, 2010, 30(2): 155 ~ 160.
- [ 8 ] Yang H Y, Guo X W, Wu G H, et al. Research progress of electrodeposition in ionic liquids [J]. International Materials Reviews, 2009, 23(3): 17 ~ 21.
- [ 9 ] 薛红,韦风云,吴庆海,等. 室温离子液体在镀层电沉积中的应用 [J]. 有色金属, 2007, 59(4): 115 ~ 117.
- [ 10 ] Abbott A P, Capper G, Davies D L, et al. Selective extraction of metals from mixed oxide matrixes using choline based ionic liquids [J]. Inorganic Chemistry, 2005, 44(19): 6 497 ~ 6 499.
- [ 11 ] Bakkar A, Neubert V. Electrodeposition onto magnesium in air and water stable ionic liquids: From corrosion to successful plating [J]. Electrochemistry Communications, 2007, 9(9): 2 428 ~ 2 435.
- [ 12 ] Abbott A P, Davies D L, Capper G, et al. Ionic liquids and their use as solvents: WO 2002026701A2 [P]. 2002-04-04. [编校: 严 灿]

# 西安华钊电子油科技有限公司

## ——新型环保电接触表面润滑保护材料

西安华钊电子油科技有限公司是专业从事电接触表面的三防、润滑、保护材料研制和销售的高新技术企业。同时代销往原优吉莱特(上海)贸易有限公司的电镀添加剂。

公司主导产品适用于各种金属和非金属的导电、非导电表面,适用于航空航天、电子、邮电、通讯、汽车、家用电器、机械加工、文物保护、首饰、工艺美术品、刀具、模具、量具、五金配件、乐器、纺织等行业。

产品通过瑞士通标准技术服务有限公司SGS检测,符合欧盟ROHS指令要求,通过许多军工、民用企业的检测和测试,实际使用效果良好。高档产品表现在:

1. 环保型产品不含1-1-1三氯乙烷,种类齐全,脂状、油性、溶剂型、水溶性型四大类。
2. 军用产品通过GJB 1217-91耐高温寿命试验,(试验温度200~203℃,时间1 000 h)。
3. 军用产品镀银工件1% K<sub>2</sub>S可通过50~300 min以上不变色,20 ppm H<sub>2</sub>S中96 h不变色。

电接触表面润滑保护剂系列产品主要功能和特点是:

**稳定接触电阻** 使电接触表面处于润润保护下,避免或极大减轻了操作使用和周围环境对其产生的不良影响,从而有效地保证电接触,且不影响电器元件的导电性、绝缘性及高频性能。

**显著的防潮、防腐蚀、防盐雾作用** 较好地解决了镀银层硫化、镀金层微孔电化学腐蚀、镀锡及其合金层的氧化等问题,有效提高有色金属表面的抗腐蚀能力,且不影响可焊性。

**良好的润滑作用** 使电接触表面之间的摩擦系数降低,

动作分离力减小,从而抑制磨损,提高了电接触表面的可靠性和使用寿命。

**降低贵重金属金、银、锡消耗的有效途径** 当镀层特别是镀金层减薄到一定厚度,并在其表面涂敷相应的润滑保护剂时,能得到与减薄前相同的效果,甚至更佳。

产品一览表

类别	脂状	油性	水溶性	溶剂型	
型号	Z-9203 各种镀层 Z-9203-1 各种镀层	YJ-9201金 YX-9202 锡合金 YT-2002铜 锡合金 G-310各种 镀层	SJ-2004金 SY-9805银 ST-2003铜 SX-2002锡 SN-2006 镍、铝、 锌合金	TL-1589 金、 银 LJ-9204 金层 LY-9205 银 LY-9308-1 银 LY-9808 银 LT-9307-1 铜 T-9807 铜、 三元合金	LX-9206 锡 LX-2006 锡 LN-9402 镍 铝锌 TL-7 各种 镀层
温度	-60~100℃、-60~120℃、-55~260℃				
单价	200~2 000 元/L或200~2 000 元/kg				

单位名称: 西安华钊电子油科技有限公司  
电话: (029)88236846 88258726  
地址: (710065)西安市电子100号信箱生产力大厦612室  
总经理: 杨双堂 13669250885  
联系人: 杨会敏 13991809567 杨会利 13609118168  
公司网址: www.xahuazhao.com  
E-mail: yanghuimin@vip.sohu.net



## Contents & Abstracts

### Influence of Current Density on Corrosion Resistance of Electroplated Zinc Coating of Magnesium Alloy Deposited from Choline Chloride-Urea Ionic Liquid

WANG Wei<sup>1,2</sup>, CHU Qing-wei<sup>1</sup>, LIANG Jun<sup>1</sup>, DAI Jian-feng<sup>2</sup> ( 1. State Key Laboratory of Solid Lubrication-Lanzhou Institute of Chemical Physics, Chinese Academy of Sciences, Lanzhou 730000, China; 2. Faculty of Science, Lanzhou University of Technology, Lanzhou 730000, China ). *Cailiao Baohu* 2013 46(08) 01~04(Ch). A choline chloride-urea ionic liquid bath was adopted to deposit Zn coating on AM60B Mg alloy. The influence of current density on the morphology and microstructure of as-plated Zn coating was investigated with a scanning electron microscope, an energy dispersive spectrometer, an X-ray diffractometer and a thickness gauge. Moreover, the corrosion resistance of as-plated Zn coating was evaluated based on measurement of electrochemical polarization curve. Results showed that the grain size of electroplated Zn coating increased with increasing current density, and the amount of pores in as-plated Zn coating declined therewith. Besides, the corrosion resistance of the Zn coating increased initially and declined later with increasing current density. Particularly, the Zn coating obtained at a current density of 5.0 mA/cm<sup>2</sup> was uniform, compact, bright, and free of defects, showing good adhesion to substrate and possessing the best corrosion resistance.

Key words: electroplated zinc coating; AM60B magnesium alloy; choline chloride-urea ionic liquid; current density; adhesion; corrosion resistance

### Effect of Silicon Dioxide Content in Low-Temperature Iron Plating Bath on Wear Resistance and Corrosion Resistance of Iron-Based Composite Coating

YANG Sen, LI Yan-li, ZHANG Na( School of Mining Technology, Liaoning University of Engineering and Technology, Huludao 125105, China ). *Cailiao Baohu* 2013 46(08) 05~07(Ch). A proper amount of SiO<sub>2</sub> as well as a small amount of MnCl<sub>2</sub> and NaCl was introduced into low-temperature iron plating bath to deposit Fe-based composite coating on the surface of mild steel (45 steel). The wear resistance, microhardness, deposition rate, and corrosion resistance of as-deposited Fe-based composite coating were measured with relevant Chinese national standard methods, and the influence of SiO<sub>2</sub> content in the plating bath on the performance of as-deposited composite coating was investigated. Results showed that the microhardness and wear resistance of Fe-based composite coating significantly rose with increasing content of SiO<sub>2</sub> in the plating bath, and the corrosion resistance of the composite coating slightly declined therewith. In the meantime, the content of SiO<sub>2</sub> in as-deposited composite coating rose with increasing content of SiO<sub>2</sub> in the plating bath; and the composite coating deposited from the plating bath containing 30 g/L SiO<sub>2</sub> had a slightly reduced deposition rate and the best comprehensive performance.

Key words: Fe-based composite coating; SiO<sub>2</sub> content; wear resistance; microhardness; deposition rate; corrosion resistance

### Comparison of Performance of Electrodeposited Lead-Silver Anode and Cast Lead-Silver Alloy Anode

ZHOU Song-bing<sup>1</sup>, GUO Zhong-cheng<sup>1,2</sup>, CHEN Bu-ming<sup>1,2</sup>, HUANG Qian<sup>1</sup> ( 1. Faculty of Metallurgical and Energy Engineering, Kunming University of Science and Technology, Kunming 650093, China; 2. Kunming Hengda Technology Company Ltd., Kunming 650106, China ). *Cailiao Baohu* 2013 46(08) 08~11(Ch). Pb-0.8% Ag anode was prepared on the surface of Al

substrate by electrodeposition. In the meantime, conventional Pb-0.8% Ag alloy anode for a comparative study was also prepared by casting. The electrochemical properties, microstructure and morphology of as-prepared Pb-Ag anodes were comparatively investigated based on measurements of galvanostatic polarization curves, cyclic voltammetry curves and electrochemical impedance spectra as well as X-ray diffraction analysis and scanning electron microscopic observation. Results showed that, as compared with conventional cast Pb-0.8% Ag alloy anode, electrodeposited Pb-0.8% Ag alloy anode was more compact and uniform, and contained a higher content of PbO<sub>2</sub>, while it possessed better corrosion resistance and electric conductivity as well.

Key words: electrodeposited lead-silver alloy anode; cast lead-silver alloy anode; electrochemical properties; corrosion resistance; electric conductivity

### Pitting Corrosion Resistance of Rare Earth Conversion Film on AZ63 Magnesium Alloy Influenced by Aging

WANG Ji-min<sup>1</sup>, CHEN Lin<sup>1,2</sup>, WANG Ning-ning<sup>1</sup>, CHEN Chang-guo<sup>1</sup> ( 1. College of Chemistry and Chemical Engineering, Chongqing University, Chongqing 400044, China; 2. College of Material and Chemical Engineering, Sichuan University of Science and Engineering, Zigong 643000, China ). *Cailiao Baohu* 2013 46(08) 12~14(Ch). AZ63 Mg alloy was immersed into the mixed solution of lanthanum nitrate and cerium nitrate to generate dual rare earth (La and Ce) conversion film. As-obtained rare earth La-Ce conversion film was then aged for different duration. The pitting behavior of the aged rare earth conversion film in 3% NaCl solution was evaluated based on measurements of cyclic voltammetry curve and polarization curve as well as observation by scanning electron microscopy. Results indicated that aging treatment helped to improve the adhesion strength to substrate, compactness and uniformity of rare earth conversion film, thereby significantly improving the corrosion resistance of the Mg alloy. Particularly, the corrosion resistance of the conversion film increased initially and then decreased with the extended aging duration. The conversion film after 48 h of aging was compact and had high adhesion force as well as good corrosion resistance, showing a breakdown potential of -1.418 V as well as shallow pitted holes. Moreover, pitting corrosion of the rare earth conversion film was more easily induced at a high current density; and it needed 480 s and 300 s to induce pitting corrosion of the rare earth conversion film under an inductive current density of 0.4 mA/cm<sup>2</sup> and 1.5 mA/cm<sup>2</sup>.

Key words: rare earth La-Ce conversion film; magnesium alloy; aging; inductive pitting; corrosion resistance

### Preparation of $\gamma$ -Glycidoxypropyltrimethoxysilane Self-Assembled Film on Stainless Steel Substrate and Evaluation of Corrosion Inhibition Performance of the Film

LI Min-ya, WANG Hai-ren, QU Jun-e, CAO Zhi-yong, CHEN Feng, NIE De-jian( Faculty of Materials Science and Engineering, Hubei University, Wuhan 430062, China ). *Cailiao Baohu* 2013 46(08) 15~17(Ch). 430 stainless steel (denoted as 430SS) was separately pretreated with two kinds of routes, and then immersed in the solution of  $\gamma$ -glycidoxypropyltrimethoxysilane (denoted as GPTMS) to generate self-assembled film. The corrosion resistance of the GPTMS self-assembled film on 430SS pretreated with two different routes was compared in association with Fourier transform infrared spectrometric analysis, electrochemical measurements, and scanning electron microscopic observation. Moreover, the influence of self-assembled time on the